MÖBIUS–INVARIANT KNOT ENERGIES

R.B. KUSNER
Department of Mathematics, University of Massachusetts, Amherst, MA, USA 01003-4515

J.M. SULLIVAN
Department of Mathematics, University of Illinois, Urbana, IL, USA 61801-2975

There has been recent interest in knot energies among mathematicians and natural scientists. When discretized, such energies can lead to effective algorithms for recognizing when two curves represent the same knot. These energies may also help model physical systems, such as long protein chains or DNA knots, subject to van der Waals interactions. Knot energies often are normalized to be scale-invariant; some important energies are also invariant under Möbius transformations of space. We describe computer experiments with such Möbius-invariant knot energies. We also discuss ways of extending these to energies for higher-dimensional submanifolds. The Appendix gives a table of computed Möbius-energy-minimizing knots and links through eight crossings. (This article is an updated version of our report[1] in *Geometric Topology*.)

1 Introduction

Is there an optimal way to tie a knot in space, or to embed a more general submanifold? And is there a natural way to evolve any embedding isotopically to an optimal one, so that we could detect whether two embeddings are isotopic?

One approach to such questions is to associate to any submanifold an energy, and look for minimizers or critical points of this energy. If the energy is infinite for immersions which are not embeddings, then presumably its gradient flow will prevent self-crossings and preserve isotopy type. One way to get an energy with an infinite barrier against self-crossings is to think of spreading charge along the submanifold and then consider the electrostatic potential. Such an energy for knots was introduced by Ohara[2] and studied by Freedman, He and Wang.[3] (A new regularization of this energy has recently been found by Brylinski.[4]) We define an analogous knot energy for k-dimensional submanifolds in n-dimensional euclidean space $\mathbb{R}^n$ (or the sphere S^n). Our knot energy is again a repulsive potential between points on the submanifold, depending only on first-order data. It is given by a regularized inverse power law, with the power chosen to make the energy scale-invariant and the regularization to make it invariant under conformal (Möbius) transformations of the ambient space.

The gradient flow of our knot energy appears to lead to optimal embeddings, both theoretically and computationally. In particular, for classical knots and links, we have used our knot energy to create an effective algorithm, implemented in Brakke's `evolver`[16], to untangle complicated curves to a simple representative for their knot type by gradient descent. In most cases, we reach the energy minimum. For instance, all unknots we have tried evolve to the round circle, and both curves in the famous Perko pair evolve to the same configuration, proving they are the same knot. Thus in most cases, this is an effective algorithm for classifying knots. However, we have also found certain links with several distinct local minima at different energy values; for these rare cases, gradient descent methods will not always reach the same final configuration.

Knot energies for curves were introduced into mathematics motivated by physical considerations; they are closely related to classically defined energies for divergence-free vector fields which arise in modeling incompressible fluid flow.[?] These new knot energies may help to model certain natural phenomena. For example, the inverse power laws in knot energies seem related to some of the energies involved in arising in protein folding problems. And recent experiments suggest that the speed of DNA knots in electrophoresis gels is correlated to other notions of knot energy.[5,6,7,8].

For surfaces, we have previously modeled[9] another Möbius-invariant energy, the elastic bending energy popularized by Willmore,[10] in the `evolver`. It is known that this energy describes the behavior of lipid vesicles, and in fact such vesicles have been observed undergoing Möbius transformations in laboratory experiments.[11] To model these vesicles in more detail, one might like to include a van der Waals interaction between different surface molecules; perhaps our Möbius-invariant knot energy would be an interesting choice for modeling such a nonlocal interaction. Our knot energies in higher dimensions or codimensions do not have obvious physical interpretation or application, although they have been useful, for example, in the topological study of knotted spheres in four-space.[12]

Our paper is organized as follows: in section 2, we define our family of knot energies for submanifolds of arbitrary dimensions. The next section explores the particular case of energies for knots and links, while section 4 discusses alternative regularizations of the knot energy. Section 5 shows why we should not expect minimizers for composite knots. We discuss the discretizations we have implemented in the `evolver`, and their success in untangling complicated unknots, in the following two sections. Section 8 relates knot energy to other measures of geometric complexity, like crossing number and ropelength. The next two sections discuss critical points for the energy which are guaranteed

../knot-ip/simtri.ps not found

Figure 1: Here $\tilde{x}$ and $\tilde{y}$ are the inversions of x and y in the sphere shown. The similar triangles prove $|\tilde{x}||\tilde{y}| \,/\, |\tilde{x}-\tilde{y}|^2 = |x||y| \,/\, |x-y|^2$. Since the conformal expansion factor for inversion from M to $\tilde{M}$ at x is $|\tilde{x}| \,/\, |x|$, the volume element changes by the k^{th} power $d\,\mathrm{vol}_{\tilde{M}}(\tilde{x}) = (|\tilde{x}| \,/\, |x|)^k d\,\mathrm{vol}_M(x)$. Combining these facts shows the integrand of our energy is Möbius-invariant.

by symmetry, and the construction in this way of Hopf links with distinct local minima for the energy. Section 11 considers the energy for higher-dimensional submanifolds in a bit more detail. Finally, we have computed energy minimizers for all knots and links up through eight crossings, and present in the last section the results of this computation and a table of their energies; our appendix shows stereoscopic pictures of the Möbius energy minimizers.

2 Defining Möbius Energies

Recall Coulomb's Law which asserts that the potential energy between a pair of unit point charges at points x and y in $\mathbb{R}^3$ is given by the reciprocal $1/|x-y|$ of their distance in space. If we imagine charge uniformly spread over a k-dimensional oriented submanifold M of $\mathbb{R}^n$, the total energy would be given by a double integral over all pairs of points on M of some inverse power of distance. Although for physical charges in $\mathbb{R}^n$ we might think of using the power $n-2$, we prefer to choose the power $2k$, which makes the integrand scale-invariant. (Without scale invariance, we would need a constraint on the size of M to get nontrivial energy minima.)

Of course, the description we have given so far ignores the fact that such an integrand will blow up as x approaches y, in such a way that the integral will be infinite for any M. So we include a regularizing factor f and define

$$E_f(M) = \iint_{M\times M} \frac{f(x,y)}{|x-y|^{2k}}\; d\,\mathrm{vol}_M(x)\, d\,\mathrm{vol}_M(y).$$

If we did not have the factor of f, this integrand clearly would be scale-invariant. In fact, it is also easy to show (see Figure 1) that it would be invariant under inversion ($x \mapsto x/|x|^2 =: \tilde{x}$), and hence under the full conformal group of Möbius transformations of $\mathbb{R}^n \cup \{\infty\}$. Note that when computing the energy, we can view M as a submanifold of $S^n \subset \mathbb{R}^{n+1}$ via stereographic projection, instead of $\mathbb{R}^n$. This follows because stereographic projection from S^n to $\mathbb{R}^n \cup \{\infty\}$ extends to a Möbius transformation of $\mathbb{R}^{n+1} \cup \{\infty\}$, and the formula for energy is independent of the ambient dimension.

Thus we would like to choose our regularizer f (which is supposed to vanish as x approaches y) to be independent of scale and also to be Möbius-invariant. We will allow this function f to depend on first-order information—the tangent planes to M at the points x and y—although this was suppressed in the notation used above.

Given a point $x \in M$ and any other point p in space, there is a unique round k-sphere $S_x(p)$ tangent to M at x and passing through p. Thus given two points x and y of M, we have two oriented k-spheres $S_x(y)$ and $S_y(x)$ which meet at equal angles at x and y. These spheres, and in particular the angle at which they meet, are defined in a Möbius-invariant manner.

By the angle between these k-spheres, we mean the angle between their tangent k-planes at points of intersection. In fact, a configuration of two oriented k-planes in $\mathbb{R}^n$ is described by k principal angles $\alpha_1, \ldots \alpha_k$, but perhaps most useful is the combined angle α whose cosine is the inner product of two simple unit k-vectors $u_1 \wedge \cdots \wedge u_k$ and $v_1 \wedge \cdots \wedge v_k$ representing the two planes:

$$\cos \alpha = \prod \cos \alpha_i = \det[u_i \cdot v_j] = (u_1 \wedge \cdots \wedge u_k) \cdot (v_1 \wedge \cdots \wedge v_k).$$

We propose taking $f(x, y)$ to be some function of these angles α_i between the spheres $S_x(y)$ and $S_y(x)$. It should be nonnegative, to keep the energy well-behaved, and should vanish when the angles are zero, in order to cancel the singularity in the integrand. We would like the energy E_f to have the following basic properties, which qualify it as a "knot energy":

- $E_f(M)$ is nonnegative, and zero only for $M = S^k$, the round k-sphere;
- $E_f(M)$ is infinite for immersions which are not embeddings, creating a barrier against M "crossing itself";
- $E_f(M)$ is finite for all compact k-dimensional embedded smooth submanifolds $M \subset \mathbb{R}^n$.

The first two properties will be true for essentially any f which is a nonnegative function of the angle α, vanishing only at 0. The third property follows if f vanishes sufficiently fast at 0 to regularize the integral.

Note that our Möbius energies $E_f(M)$ are somewhat like "quadratic forms" on the space of oriented submanifolds. We can also examine the associated "bilinear form" $E_f(M, N)$, given by the double integral over $M \times N$. If we interpret M and N as chains or integral currents, then indeed this cross-energy will be linear in each argument, but only for positive multiples. We can think of the first submanifold M defining a potential P_M^f at all points of space. Then $E_f(M, N)$ is just the integral of this potential over the points of N. Since f

depends on the tangent planes of M and N, the potential P_M^f is a function not merely of points in space, but of k-vectors at those points. In the language of geometric measure theory, P_M^f is a parametric integrand, and in fact we might think of E_f as given by a bilinear parametric integrand.

3 The Excess-Length Picture and a Standard Choice of Regularization

One good choice for the regularization in the energy E_f is $f_0 := (1 - \cos\alpha)^k$. For the remainder of this paper, we will study mostly this particular energy; we will write simply E for the energy E_{f_0} with this choice of f. This energy E generalizes the energy $\tilde{E}$ for knots $K \subset \mathbb{R}^3$ studied by O'Hara[2] and by Freedman, He and Wang:[3]

$$\tilde{E}(K) = \iint_{K\times K} \left(\frac{1}{|x-y|^2} - \frac{1}{d_K(x,y)^2} \right) ds_K(x)\, ds_K(y),$$

where $d_K(x,y)$ is the shorter arclength distance within K from x to y. In fact, Peter Doyle and Oded Schramm[13] introduced, in the one dimensional case, the idea of a regularization by a multiplicative factor depending on angle, and observed that $E(K) = \tilde{E}(K) - 4$ when the factor used is $f_0 = (1 - \cos\alpha)$. (Recently, Brylinski[4] has proposed another regularization: if we define

$$B_s(K) = \iint_{K\times K} |x-y|^s\, ds_K(x)\, ds_K(y),$$

then this function of a complex number s can be meromorphically continued from the right halfplane to the entire plane, and Brylinski shows that it has poles only at the negative odd integers, and thus in particular not at $s = -2$. It turns out that $B_{-2}(K) = \tilde{E}(K) - 4 = E(K)$.)

One way Doyle and Schramm explained the equivalence of E and $\tilde{E}$ is through a picture which interprets the potential $P_K(x) := P_K^{f_0}(x)$ as an excess length. Given a curve K in S^n, we want to evaluate P_K on a tangent direction at some point $x \in S^n$. To compute this, rotate the sphere so that x is at the north pole, and then stereographically project to $\mathbb{R}^n$ (sending x to infinity). Rotate this euclidean space so that the given tangent direction at x becomes the vertical direction. (Figure 2 shows this in the case $n = 2$, when we are projecting a curve from the two-sphere to the plane; although here all embedded curves are unknotted, the energy still makes sense.) If $\sigma(K)$ is the stereographic projection of the curve K, then we can check that $P_K(x)$ equals the integral $\int_{\sigma(K)} (1 - \cos\alpha)\, ds_{\sigma(K)}$, where in this picture the angle α is simply

../knot-ip/sphereA.ps not found (a)

../knot-ip/sphereB.ps not found (b)

Figure 2: The excess-length picture shows how to calculate the potential $P_K(x)$ for a curve K in the sphere. When we apply the stereographic projection σ (from x as north pole) the spheres $S_x(y)$ and $S_y(x)$ become straight lines at angle α. The integral of $1 - \cos\alpha$ is the excess length of $\sigma(K)$ over that of the straight line.

the angle that the tangent to $\sigma(K)$ makes with the vertical. (Our stereographic projection is scaled nonstandardly, to take the equatorial sphere to a sphere of half the size; the extra factor of $1/2$ is needed because we want to use an inversion in a unit sphere in $\mathbb{R}^{n+1}$.)

If K is a closed curve, and x is not on K, this integral is simply the length of $\sigma(K)$, because the $\cos\alpha$ term integrates to zero. Thus the potential at points not on K does not depend on tangent directions, and in fact is the same as it would be if we used no regularization, setting $f = 1$. Integrating along a second, disjoint curve L, we see that the cross energy $E(K, L)$ equals the unregularized energy $E_1(K, L)$. (This is what Dave Auckly and Lorenzo Sadun[14] refer to as the additive link property for the energy E.)

But of course for x on K, we need the regularization, as $\sigma(K)$ is an infinite curve in $\mathbb{R}^n$, asymptotic at either end to a vertical line. Notice that the difference between the length of the curve $\sigma(K)$ and its vertical progression is given by the integral of $1 - \cos\alpha$, which gave the potential P_K. Each term is infinite, but their difference is the excess length of $\sigma(K)$ compared with the vertical straight line, which is finite if K is smooth enough at x.

One might hope to use the same picture to define energies for k-dimensional submanifolds. If a submanifold M is stereographically projected from a point $x \in M$, the image is asymptotic at infinity to a flat k-plane. However, this image submanifold has infinite excess area when compared to this k-plane, since its distance from the k-plane varies as we approach infinity in different directions (unless x is an umbilic point of M). Thus a naïve definition of energy in terms of excess area will not work; in other words the energy $E_{(1-\cos\alpha)}$ is not finite for dimensions $k > 1$. Our choice of $f_0 = (1 - \cos\alpha)^k$ overcomes this difficulty, although we do not have an equally nice geometric picture for the resulting energy E.

4 Other Möbius-Invariant Knot Energies

The Möbius energy E has been useful—theoretically, and from the perspective of computer experiments—but other Möbius-invariant knot energies are possible. First we might consider another regularizer f in our general energy E_f.

Discussions with Doyle, Schramm, and Bill Thurston have focused our attention on $f = |\sin\alpha|$ as giving an interesting energy for curves. One problem here is that f is not differentiable, so E_f does not have a well-behaved gradient flow, and it is hard to model numerically. Higher powers of this function give regularizers for k-submanifolds; perhaps in this case there are further good choices for f.

Our E_f is defined in terms of first-order information at the two points x and y in the double integral. If we allow the use of higher-order information, there are other possibilities for the regularization. For two-dimensional surfaces, Auckly and Sadun[14] have suggested a regularization using the squared-mean-curvature integral (which is second-order data), but this is difficult to bound below.

We have also proposed a "holomorphic" energy for embedded Riemann surfaces by considering a relative energy within conformal classes. We choose a reference embedding of a surface in space; then the energy of any conformally equivalent embedding is given by comparing the straight-line distance between a pair of points on the surface with the corresponding distance on the reference surface. We have yet to find a proper regularization for this energy, but for spheres there is of course a unique conformal class, and the round sphere serves as a natural reference surface. This idea of relative energy should extend to rather general subsets of $\mathbb{R}^n$, and in fact we have already succeeded in regularizing it for embedded 1-complexes or "knotted graphs"[15].

5 Prime Decomposition

We are interested in minimizing E_f within isotopy classes. Given a submanifold $M \subset \mathbb{R}^n$, we write $[M] = \{N\colon\ N \sim M\}$ for its isotopy class, and

$$E_f([M]) = \inf_{N\sim M} E_f(N)$$

for the infimum energy. One basic result[3] is that prime knot types have E-minimizing representatives—this infimum is achieved. On the other hand, it seems that under energy minimization, composite knots decompose into their summands in a natural way. More generally, given a pair of k-dimensional submanifolds M and N, there are two ways to naturally combine or add their isotopy classes $[M]$ and $[N]$, in such a manner that minimizing the energy seems to separate the two pieces again.

Most trivial is the disjoint union $[M]\sqcup[N]$, obtained by embedding M and N in disjoint balls in $\mathbb{R}^n$. It is clear that by placing M and N far apart from each other (or equivalently scaling each one down) we can make their cross-energy $E_f(M,N)$ arbitrarily small. Since the energy of the union is the sum

../knot-ip/ears.ps not found

Figure 3: After applying Möbius transformations to Q in $[M]$ and R in $[N]$ to get large round pieces, we can weld them together to make this representative for $[M]\#[N]$, with energy not much more than $E_f(Q) + E_f(R)$.

of the self-energies and the cross-energy, it is thus clear that

$$E_f\big([M]\sqcup[N]\big) = E_f\big([M]\big) + E_f\big([N]\big).$$

Even a submanifold of several topological components may not be decomposable in this way as a disjoint union; in this case we say it is essentially linked.

There is also a natural notion of the connected sum $[M]\#[N]$, which is well defined when M and N are both connected. (Of course, if M or N has more than one component, we simply must specify which components are to be connected.) We say a submanifold is prime if the only way it can be decomposed as a connected sum is when one summand is isotopic to a trivial S^k. Using Möbius invariance, we find that

$$E_f([M]\#[N]) \leq E_f([M]) + E_f([N]).$$

To check this, consider $Q \sim M$ and $R \sim N$ each having E_f within any given $\varepsilon > 0$ of the respective infimum values. Deform a small neighborhood of some point on Q to be flat, changing the energy only by ε, and then apply a Möbius transformation mapping this small piece of a k-plane to almost all of a round S^k. Apply the same procedure to some point on R. Welding the resulting submanifolds together in the obvious way, we get a submanifold P in the class $[M]\#[N]$ (resembling a round k-spherical "head" with copies of Q and R attached as small "ears"—see Figure 3) with

$$E_f(P) \leq E_f(Q) + E_f(R) + 3\varepsilon,$$

where the last ε includes the interaction terms between the two "ears". Infimizing yields the desired inequality.

In fact, we conjecture equality holds for infima of the energy E, and moreover, that minimization of E leads to a natural "conformal connected sum decomposition" of a submanifold into E-minimizing, essentially linked, prime submanifolds. This phenomenon has been observed in our computational investigations of the energy E for knots, links and surfaces in $\mathbb{R}^3$, described in the next section. Figure 4 shows what we expect is a minimizing sequence for the energy of a connected sum of two trefoil knots. (Note that we consider left- and right-handed trefoils to be distinct isotopy classes, and that this matters when taking connected sum. Of course they have the same energy, so are not considered separately in our later knot tables.)

../knot-ip/npA.ps not found (a)

../knot-ip/npB.ps not found (b)

Figure 4: We expect that an energy-minimizing sequence for this "square knot" type, the connected sum of a left-handed and a right-handed trefoil knot, will begin as above. The knot (a) has energy approximately 150, while (b) has energy approximately 142. The limit energy of the sequence is approximately 140.824, or exactly twice the energy of the critical trefoil of Section 9.

6 Discretization and Computer Experiments

In order to gain some intuition into the behavior of the Möbius energy, especially for knots and links, we have implemented various discretizations of E and its gradient flow, and carried out computer experiments using Brakke's `evolver`. All our discrete models work with polyhedral surfaces or polygonal knots and links. These have infinite energy E, since they have sharp corners, so we must work with some discretization of the energy, which is supposed to model the energy of a nearby smooth curve or surface.

One discretization for curves, the *cosine energy*, places point charges at the midpoints of all edges of the polygon. The charge at x equals the length l_x of the edge. For this energy, we sum $(1-\cos\alpha)l_x l_y/|x-y|^2$ over all pairs $x \neq y$; here α is the angle between two circles passing through the midpoints x and y. In fact, α can be more easily computed as the angle between the edge at x, and the edge at y reflected in the perpendicular bisector of $\overline{xy}$ (so that it also passes through x).

If we approximate some smooth curve by polygonal segments, this discretization seems to give energy values quite close to the true energy of the smooth curve, even when the polygonal approximation is relatively coarse. However, its gradient flow is problematic, since some edges tend to get very short, and then sometimes fail to line up with their neighbors. We can avoid this problem by adding a "Hooke" term to the energy, which tends to keep all the edges in the polygon at some fixed length by pretending the edges are stiff springs with that equilibrium length.

The *edge energy* discretization is the same, but without the $(1-\cos\alpha)$ factor in the summand. This models the unregularized energy E_1, but of course the discrete sum is finite. The idea is that if we wrote down a discretization for the formula for $\tilde{E}$, the regularization term would depend only on the edge lengths of the polygon, and not on its position in space. This subtracted term in fact is smallest when the edge lengths are equal, so leaving it out of the energy we minimize simply helps keep edge lengths equal (as the Hooke energy did). Note also that the exact integral of $1/|x-y|^2$ over a pair of disjoint

Number of edges	80	160	320	640
Cosine energy	70.85	70.52	70.44	70.42
Edge energy	72.24	71.21	70.79	70.59
Vertex energy	69.16	69.84	70.14	70.28

Table 1: These discrete energies were computed for minimal polygonal trefoil knots with equal edge lengths in S^3, approximations to the symmetric critical trefoil whose true energy $E \approx 70.41204$ is computed in Section 9.

line segments in space is not an elementary function of their endpoints; this is why we concentrate the charges at the edge midpoints in the edge and cosine energies.

Finally, the *vertex energy* places a charge at each vertex v of the polygonal knot. The charge l_v equals the average of the adjacent edge lengths. Again we merely sum $l_v l_w/|v-w|^2$ without any regularization. This vertex energy is the one we have used for most of our gradient flows. For informational purposes, we also compute the sum of $l_v l_w/d^2(v,w)$, which is subtracted from the vertex or edge energies as a regularization. We report the values of all three discretized energies for our final knots. All three seem to converge as the number of segments used increases, though the cosine energy is by far the most accurate. Table 1 reports these energies computed for polygonal approximations to the critical trefoil knot whose energy can be computed exactly (see Section 9).

There have been some previous experiments with the energy $\tilde{E}$ by other researchers: Kazushi Ahara[17] has used a method like our vertex energy with Hooke terms to compute several simple examples, and a program of Steve Bryson[18] was able to approximate the minimal trefoil. Others, including Buck, Orloff and Simon,[19,20] Fukuhara,[21] and Gunn,[22] have done experiments with other repulsive energies for explicitly polyhedral knots; some of these do not model any energy for smooth knots. Since our experiments were first reported, some other groups[23,24] have suggested using simulated annealing to find global minimizers for knot energies. We have not found that to be necessary, as the simpler gradient descent methods almost always lead to the global minimum.

Of course, the vertex-based discretization (by which we flow) does not have an infinite barrier to changing knot type. Two segments can cross each other in space if their endpoints stay far away. But in practice, this does not happen as long as we keep edge lengths short enough near tight crossings. We can do this either with the Hooke energy, forcing all edges to be short, or by selectively refining edges whose contribution to the knot energy has become large during the evolution. The latter method seems preferable, as it concentrates the

../knot-ip/treftube.ps not found

Figure 5: This torus, in the isotopy class of a tubed trefoil knot, seems to minimize energy, with $E \approx 638$. In S^3, it would evidently be the orbit of a small circle under a rigid rotation.

vertices where they are needed, and in the case of links does not constrain the relative lengths of the components. As always, we view our polygons as approximations of smooth curves; this "retriangulation" merely maintains a good approximation.

As always with the `evolver`, formulas for the exact gradients of the discrete energies are programmed into the computer code. Thus, at any given configuration the gradient is known exactly (without testing different perturbations) and the conjugate gradient method is used to flow towards a critical point.

We have also implemented some discretizations of energies for surfaces of dimension two, though not for submanifolds of arbitrary dimension. Here, one discretization is like the vertex energy, ignoring regularization and placing a charge at each vertex equal to one third of the area of the surrounding triangles. This energy seems to work nicely for surfaces in $\mathbb{R}^4$, but for surfaces in $\mathbb{R}^3$ it is too rigid: the high power in the $1/r^4$ repulsive energy (needed for surfaces) means that vertices are influenced mostly just by their nearest neighbors. Thus the discrete surface seems to get locked into a particular, nearly equilateral triangulation, without much freedom to move. It is also not clear if this energy models any E_f.

For surfaces in space, we have had more success with a discretization of the $(1-\cos\alpha)^2$ energy which places a charge at the center of each face, equal to its area, and computes the angle between the tangent planes at pairs of faces. We have computed, for instance, a tube around a trefoil knot (see Figure 5) with energy about 638, but we have yet to do comprehensive experiments with this energy. As with the similar cosine energy for links, we must pay special attention to keep the triangulation from degenerating during the evolution. Dennis Roseman [12] has made use of both of our discretizations for surface energies to simplify knotted and unknotted surfaces in four space.

7 Untangling Unknots

For any prime knot type, the existence of an E-minimizer is guaranteed by the result of Freedman, He and Wang [3] already mentioned. But this leaves open the interesting question of whether the same knot type might have other critical points for E, and in particular further local minima. Of course, the

../knot-ip/unknotA.ps not found
(a)

../knot-ip/unknotB.ps not found
(b)

../knot-ip/unknotC.ps not found
(c)

../knot-ip/unknotD.ps not found
(d)

Figure 6: The tangled unknot (a) quickly rounds off to the smooth curve (b). Eventually loops grow as needed to swing out around the knobs, giving the curve (c), which can then shrink these loops to pull them through. The curve (d) clearly has no further obstacles to becoming a round circle, and indeed quickly evolves there.

E-gradient flow will be most useful for classifying knots if no other minima exist.

Of special interest are tangled unknots. There is no efficient algorithm known for untangling an unknotted curve, though according to Hatcher's solution[25] of the Smale Conjecture, there is no obstruction to finding a flow which evolves any unknotted curve to a round circle. We would be surprised if the E-flow accomplished this, but we were equally amazed to see that the (discrete) flow did untangle the example[3] in Figure 6. Although initially the evolution seems to lead to a large loop caught in a tight slip-knot, perhaps it is the Möbius invariance which lets different parts of the curve grow or shrink as necessary to untangle the unknot to a round circle. The full process is shown in our six-minute video,[26] along with other examples of evolutions towards E-minimizing knots and links.

Of course, our experiments showing how this one curve untangles leave open the basic question: are there any E-critical unknotted curves besides the round circle? A negative answer would give an elegant analytic proof of Hatcher's theorem.

8 Crossing Numbers and Ropelength

Knots and links are often studied by means of planar projections with marked crossings. Any two projections of equivalent knots can be obtained from each other by a sequence of Reidemeister moves.[27] The topological crossing number $c([K])$ of the link type $[K]$ is defined as the minimum number of crossings in any planar projection.

From a three-dimensional geometric perspective, perhaps more interesting is the average crossing number $A(K)$ of the space curve K, which is the average number of crossings in planar projections of the curve, averaged over all

possible orthogonal projections. This can be computed by a formula of Gauss:

$$4\pi A(K) = \iint_{K\times K} \frac{|(u\times v)\cdot(x-y)|}{|x-y|^3}\, ds_K(x)\, ds_K(y),$$

where u and v are the unit tangent vectors to K at x and y, respectively. In our computations, we discretize this for a polygonal link as a double sum over all pairs of edges, using the edge vectors for u and v, and the edge midpoints for x and y. It is clear that $A(K) \geq c([K])$ for any link.

One result of Freedman, He and Wang[3] is a relation between the energy E and the crossing number, namely $E(K) \geq 2\pi c([K])$. This follows from a similar relation between the energy of any curve and its average crossing number, once we apply a Möbius transformation to send one point of the curve to infinity. They also show that $E(K) \geq \frac{6}{11} 2\pi A(K) - \frac{56}{11}$. They prove these results only for knots, although it is easy to check they remain true for our link energy. Note, in this context, their normalization of the energy for links different from ours: they count cross terms between different components only half as much as the self-energy terms. We believe our normalization is more natural, providing a good ordering of all links by energy, independent of how many components they have.

Another scale-invariant (but not Möbius-invariant) geometric measure of the complexity of space curve K is its ropelength $L(K)$, which is the arclength divided by "thickness"—essentially the diameter of the biggest embedded tubular neighborhood.[28,29] It is known[30,8,31] that $A(K) \leq CL(K)^{4/3}$ for a universal constant $C \leq 1/4$, and similarly[32] that certain energies similar to ours are also at most $L(K)^{4/3}$ times a constant. It would be interesting to prove this for the Möbius energy.

Since the standard projection of any knot type has a minimal number of crossings, we usually like to reduce any projection of that knot to the standard one only using Reidemeister moves which decrease the number of crossings. But sometimes this is impossible. The projection of our initial curve shown in Figure 6(a) has 32 crossings, and it is easy to check that no moves are applicable except the ones which increase crossing number. It seems that at least four extra crossings must be introduced to move this diagram to the zero-crossing picture of the unknot. Therefore, before our experiments, it was reasonable to think that the corresponding three-dimensional (but nearly planar) example might not untangle under the E-flow.

../knot-ip/35A.ps not found (a)

../knot-ip/35B.ps not found (b)

Figure 7: The E-critical orbital $(3, 5)$ torus knot (a), with energy just over 265, is not stable, while the knot (b), with energy numerically computed to be slightly under 260, seems stable and presumably is the minimizer.

../knot-ip/helix.ps not found

Figure 8: This double helix, critical for E, is a limit of minimizing $(2, q)$ torus knots for large q; many knot minimizers seem to include segments which look like a piece of this helix. We show a stereo pair of pictures; to see the stereoscopic effect, look at one figure with the left eye and the other with the right eye (either by crossing the eyes or by straightening them, perhaps with the aid of a stereo viewer).

9 Critical Knots and Links from Group Actions

One can also ask about the existence of further critical points for truly knotted curves. Perhaps the simplest of these are the (p, q) torus knots and links. These curves can be realized as (unions of) orbits of points under rigid rotations of S^3, which rotate one two-plane at speed p and the perpendicular one at speed q. (These rotations can also be viewed as Möbius circle actions on $\mathbb{R}^3 \cup \infty$.) In earlier work with Denise Kim,[33] explicit E-critical torus knots and links were constructed, by varying the ratio of radii of the torus containing these orbits until we reach a critical ratio, then using the "principle of symmetric criticality".

Once we have reduced the energy to a function on the space of orbits (which is finite dimensional, and in this case can be parametrized by the ratio of radii), this principle asserts that at a critical point of the reduced energy, the corresponding knot or link is critical for E among *all* variations. To see this, note that if the gradient of E did not vanish, we could simply average it over the orbit to get a variation through orbits which changed (to first order) the reduced energy, contradicting the fact that we are at a critical point on the orbit space.

It can be shown[15] that for large p and q (each at least 3) these orbital (p, q) torus knots and links are unstable for E (compare Figure 7), hence they are not the E-minimizers which are guaranteed to exist by the direct method.[3] In particular, there is more than one critical point for E within each of these isotopy types. On the other hand, the orbital $(2, q)$ torus knots do appear to be the E-minimizers, at least experimentally; as $q \to \infty$, these converge to an E-critical double-helix (see Figure 8) whose pitch, close to 1.454, is a universal constant.

../knot-ip/t23A.ps not found
(a)

../knot-ip/t23B.ps not found
(b)

../knot-ip/t23C.ps not found
(c)

../knot-ip/t23D.ps not found
(d)

Figure 9: All these are views of the same critical trefoil, the presumed energy minimizer, differing only by Möbius transformations. The view (a), which is a different planar projection of the same space curve shown in the Appendix, is a $(2,3)$-torus knot in space, while (b) is dually a $(3,2)$-torus knot. The view (c) shows how any curve can be shown as a large circle with a small "ear", while (d) is a randomly chosen view.

The energies of these orbital critical points can be computed by an analytic formula, derived with Gil Stengle.[33] This is obtained by using the circle action to reduce the double integral for E to an explicit single integral of a meromorphic differential around the unit circle $S^1 \subset \mathbb{C}$, and evaluating this as a residue sum. For example, the critical trefoil (or $(2,3)$ torus knot, see Figure 9) has Möbius energy

$$E = 4\pi^2 \min_r (4r^2 + 9) \sum \mathrm{Res} \frac{-z^2}{r^2 z(z^2-1)^2 + (z^3-1)^2} \approx 70.41204,$$

where the sum is over poles within the unit circle, and the minimum is achieved at $r \approx 1.857$.

10 Hopf Links and Electrons on S^2

We can find more examples of links with several E-critical points, and presumably several local minima, by examining the special case of Hopf links with the methods of the previous section. Recall that the Hopf fibration of S^3 is given by the orbits of the usual action of $S^1 \subset \mathbb{C}^*$ on $S^3 \subset \mathbb{C}^2$. Each fiber is a great circle, and each pair of fibers has linking number 1. We call the union of any p fibers a p-component geometric Hopf link; for a given p, all such links are isotopic. We can find E-critical points for this link type among such geometric Hopf links by lifting a finite set of points from S^2, the orbit space for the Hopf action.

Explicitly, suppose that in our p-component Hopf link $(\Gamma_1, ..., \Gamma_p)$, each component Γ_j corresponds to the point x_j on S^2. Then we can compute

$$E(\Gamma_1, ..., \Gamma_p) = 4\pi^2 \sum_{i \neq j} \frac{1}{d_{ij}},$$

where $d_{ij} = |x_i - x_j|$ is the straight-line distance in $\mathbb{R}^3$ between the points x_i and x_j. In other words, the Möbius energy of a geometric Hopf link is simply (a

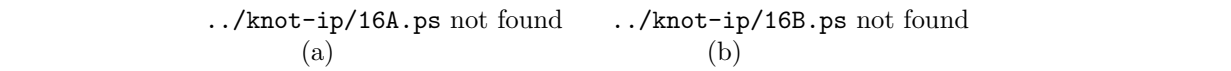

(a) (b)

Figure 10: Two stable configurations of sixteen point charges on the sphere, shown with the closest pairs joined with edges. Configuration (a) has tetrahedral symmetry and lower energy; configuration (b) has amphichiral D_8 symmetry and slightly higher energy.

multiple of) the ordinary Coulomb energy of the corresponding point charges in $\mathbb{R}^3$ constrained to lie on the round sphere. Thus, in this case, the residue sum for E has a simple geometric interpretation; it would be interesting to know whether this interpretation could be extended beyond Hopf links to torus knots and links.

When the number of components p is less than 4, it is easy to see that there is only one critical configuration of charges on S^2 (or thus of Hopf circles in S^3). This is the global minimum for the Coulomb energy, with the points spaced equally around the equator, corresponding to (p, p) torus links. But when $p = 4$ there are two distinct critical configurations: the equatorial configuration (or geometric $(4, 4)$ torus link) is an unstable equilibrium, while the global minimum has points at the vertices of a regular tetrahedron (the link having fallen off the torus in S^3).

In the early part of this century, just before the discovery of quantum mechanics, there was interest in this problem, because it was thought that stable configurations of electrons on a sphere might explain the periodic table of elements. With this in mind, configurations of $p \leq 8$ points were analyzed in detail by Föppl.[34]

To examine the structure of critical geometric Hopf links in general, consider a variation which moves each of the corresponding points x_i by Δx_i, and set $u_{ij} = (x_i - x_j)/d_{ij}$ and $v_{ij} = (\Delta x_i - \Delta x_j)/d_{ij}$. Then to second order, the change in energy is

$$\Delta E = 2\pi^2 \sum_{i \neq j} \frac{1}{d_{ij}} \left(2v_{ij} \cdot u_{ij} - v_{ij} \cdot v_{ij} + 6(v_{ij} \cdot u_{ij})^2 \right).$$

Of course, if the points x_i are to remain on S^2, we must also impose on the variation the constraint $\Delta x_i \cdot x_i = 0$ for $i = 1, ..., p$.

We have done extensive numerical experiments to find such stable configurations of p point charges on S^2. These indicate that for $p < 16$ there is a single minimum. When $p = 16$ there seem to be two stable configurations, shown in Figure 10. One has tetrahedral A_4 symmetry of order 12 and $E \approx 7336.010$; the other has amphichiral dihedral D_8 symmetry of order 16 and $E \approx 7336.697$; the first local minimum seems to attract about three-quarters of the random

configurations we start with. For configurations of greater numbers of points, not surprisingly there are again usually distinct local minima.

Our experiments also suggest that the corresponding geometric Hopf links are Möbius-energy stable. Thus, the 16-component Hopf link gives the first known example of a link type with distinct local minima for the knot energy E. In general, we conjecture that the Morse index for an equilibrium configuration of point charges equals that of the corresponding geometric Hopf link. The configuration space of distinct points on S^2 has plenty of cohomology, so we expect to find many unstable extrema by viewing the reduced energy as an equivariant Morse function.[35] (In this context, Kawazumi[36] has investigated critical points of a logarithmic repulsive potential.)

11 Surfaces and Submanifolds

In the case of surfaces and higher dimensional submanifolds, we know much less about the existence of E-stationary examples or E-minimizers. Presumably, for instance, the round S^2 is the unique critical point for spheres in $\mathbb{R}^3$ (again consistent with the Smale Conjecture), and prime knotted spheres in $\mathbb{R}^4$ have E-minimizing representatives.

Using a simple scaling argument we are able to prove some partial regularity results in general dimensions. For example, tangent cones (if they exist) to k-dimensional submanifolds with finite E must be flat k-planes.[15] Presumably E-minimizers have tangent cones everywhere, from which it follows that they are at least C^1 submanifolds; in fact, we expect all E-minimizers to be real analytic submanifolds.

To explicitly compute the energy E of a submanifold it is helpful to rewrite the formulas for the angle α. If two points x and y on $M \subset \mathbb{R}^n$ are separated by the vector $r = x - y$, and the tangent spaces to M at these points are spanned by $s_1, s_2, \ldots, s_k$ and by $t_1, t_2, \ldots, t_k$, then we do not have to find the spheres $S_x(y)$ and $S_y(x)$ in order to determine how they meet. Instead, note that $S_x(y)$ is tangent to M at x, while the tangent space to $S_y(x)$ there is obtained by reflecting the tangent space $T_y(M)$ in the vector r, and is thus spanned by the vectors $\bar{t}_i := t_i - 2(r \cdot t_i)r/r^2$. Observe that the $\bar{t}_i$ have the same inner products with each other as the t_i do; however, this basis for the tangent space to $S_y(x)$ has the wrong orientation, because of the reflection.

Define a $(k+1) \times (k+1)$ matrix A by setting $A_{00} := r^2/2$, $A_{0j} := r \cdot t_j$,

$A_{i0} := s_i \cdot r$, $A_{ij} := s_i \cdot t_j$. Thus we have

$$A = \begin{pmatrix} r^2/2 & \dots & r \cdot t_j & \dots \\ \vdots & \ddots & \vdots & \\ s_i \cdot r & \dots & s_i \cdot t_j & \dots \\ \vdots & & \vdots & \ddots \end{pmatrix}.$$

By row reduction applied to the leading row and column of A, we find $\det A = \frac{r^2}{2} \det[s_i \cdot \bar{t}_j]$. This latter determinant is the one used to find $\cos\alpha$, so we get

$$\frac{-r^2}{2} \cos\alpha \left|s_1 \wedge \cdots \wedge s_k\right| \left|t_1 \wedge \cdots \wedge t_k\right| = \det A,$$

where the minus sign comes from the reversal of orientation by the reflection.

Note that by choosing principal angles we can arrange the s_i and t_j to be orthogonal sets of vectors with the property that $s_i \cdot t_j = 0$ unless $i = j$. Then the formula above simplifies to

$$\frac{-r^2}{2} \cos\alpha \prod_{j=1}^{k} |s_j||t_j| = \left(\frac{r^2}{2} - \sum_{j=1}^{k} \frac{(s_j \cdot r)(r \cdot t_j)}{s_j \cdot t_j}\right) \prod_{j=1}^{k} s_j \cdot t_j. \tag{1}$$

As an example, let us compute the energy of a k-dimensional Clifford torus of radii $r_1, \dots, r_k$. We have

$$T^k = S^1(r_1) \times \cdots S^1(r_k) \subset S^{2k-1} \subset \mathbb{C}^k,$$

parameterized by the map $f(\theta_1, \dots, \theta_k) = (r_1 e^{i\theta_1}, \dots, r_k e^{i\theta_k})$. This embedding is homogeneous, so the energy density is constant; thus we can compute $E(T)$ with a single integral over T:

$$E(T) = \iint_{T \times T} \left(\frac{1 - \cos\alpha}{r^2}\right)^k dx\, dy = \mathrm{vol}(T) \int_T \left(\frac{1 - \cos\alpha}{r^2}\right)^k dx \tag{2}$$

for any fixed y, say $y = f(0, \dots, 0)$. We find it easier, though, to compute this integral not by fixing this y and letting $x = f(\phi_1, \dots, \phi_k)$ vary, but by rotating so that $x = f(\theta_1, \dots, \theta_k)$ and $y = f(-\theta_1, \dots, -\theta_k)$, where $2\theta_j = \phi_j$. The tangent vectors at these points x and y are $s_j = (0, \dots, 0, ir_j e^{i\theta_j}, 0, \dots, 0)$ and $t_j = (0, \dots, 0, ir_j e^{-i\theta_j}, 0, \dots, 0)$. Their difference vector is $r = x - y = 2i(r_1 \sin\theta_1, \dots, r_k \sin\theta_k)$.

../knot-ip/clifford.ps not found

Figure 11: The minimal Clifford torus in S^3, shown stereographically projected to $\mathbb{R}^3$, has energy $E = 5\pi^3/3$, presumably the lowest of any nonspherical surface.

It is a simple matter to compute the inner products:

$$s_i \cdot s_j = t_i \cdot t_j = \delta_{ij} r_j^2, \qquad s_i \cdot t_j = \delta_{ij} r_j^2 \cos\phi_j,$$

$$s_j \cdot r = t_j \cdot r = r_j^2 \sin^2\theta_j,$$

$$r \cdot r = 4\sum r_j^2 \sin^2\theta_j = 2\sum r_j^2(1-\cos\phi_j).$$

Define an angle ϕ by $\cos\phi = \prod \cos\phi_j$. Then using the formula (1) for $\cos\alpha$, we find that

$$\cos\alpha = \cos\phi \, \frac{\sum r_j^2(1/\cos\phi_j - 1)}{\sum r_j^2(1-\cos\phi_j)},$$

which gives

$$\frac{1-\cos\alpha}{r\cdot r} = \frac{1}{2}\,\frac{\sum r_j^2(1-\cos\phi_j)(1-\cos\phi/\cos\phi_j)}{\left(\sum r_j^2(1-\cos\phi_j)\right)^2}.$$

For $k = 2$ we can now explicitly evaluate the integral (2). We find

$$\begin{aligned}
E(T) &= \operatorname{area}(T)\int_0^{2\pi}\int_0^{2\pi}\left(\frac{1-\cos\alpha}{r\cdot r}\right)^2 r_1 d\phi_1\, r_2 d\phi_2 \\
&= 4\pi^2 r_1^2 r_2^2 \int_0^{\pi}\int_0^{\pi}\left(\frac{(r_1^2+r_2^2)(1-\cos\phi_1)(1-\cos\phi_2)}{\left(r_1^2(1-\cos\phi_1)+r_2^2(1-\cos\phi_2)\right)^2}\right)^2 d\phi_1\, d\phi_2 \\
&= \frac{2\pi^2 r_1^2(r_1^2+r_2^2)^2}{r_2}\int_0^{\pi}\frac{\sqrt{1-\cos\phi_2}\left(r_1^2+3(1-\cos\phi_2)r_2^2\right)}{\left(2r_1^2+(1-\cos\phi_2)r_2^2\right)^{\frac{7}{2}}}\, d\phi_2 \\
&= \frac{\pi^3}{6}\,\frac{3r_1^4+14r_1^2r_2^2+3r_2^4}{r_1 r_2(r_1^2+r_2^2)}.
\end{aligned}$$

This is a rational function of the r_j, homogeneous of degree 0. It has a global minimum at $r_1 = r_2$, corresponding to the minimal Clifford torus in S^3, the lift of the equator under the Hopf map. We conjecture that this surface (see Figure 11) has the minimum Möbius energy for any unknotted torus in S^3; its energy is $5\pi^3/3$. In fact, this should be the absolute minimum for E among all nonspherical embedded surfaces in S^3 (or $\mathbb{R}^3$).

By the technique of symmetric criticality mentioned earlier, we do know that this surface is a critical point for E; and for any k, in fact, the k-torus of equal radii in S^{2k-1} is a critical point for the k-dimensional energy E.

12 A Table of Knots and Links Minimizing Möbius Energy

We have computed experimentally (with help from a group of undergraduate students at the Five Colleges Geometry Institute [37]) what seem to be E-minimizers for all the essential prime knots and links with less than nine crossings; these are pictured in the Appendix. Most of these knots have a two-bridge or rational tangle decomposition into segments where two particular strands twist around each other a certain number of half-turns. [38] This decomposition seems to be reflected in the shapes of the energy minimizers: each twisted piece resembles several half-turns of the E-critical double-helix (see Figure 8), up to Möbius transformations (which can send a half-turn of the helix into a pair of large arcs near infinity). It would be nice to prove that this is the shape of a minimizer, but at present it is not even known whether, for instance, a minimizer is a real analytic curve.

We computed an approximation to each knot or link by evolving at least 9000 steps with the conjugate gradient method, refining as necessary when edges had high energy. We included all the knots and links through eight crossings as well as a few nine-crossing knots and the $(2, 15)$ torus knot.

In Table 2, the first column lists the name of the knot or link from the standard tables [39] and its Conway notation. [40] The next three columns list the energy of our approximate minimizer, computed with each of the three discretizations. Finally, we list the average crossing number, and the number of edges for this polygonal link. Note that the average crossing number would change somewhat if we applied a Möbius transformation to our link, though the other values should stay constant. If we started with a different initial configuration, we might get to the same minimizer in a different picture, and the value shown for A would be different.

We believe that the cosine energy is significantly more accurate than the other discretizations, and have ordered the table by its values. Note that the edge energy tends to be a bit higher, and the vertex energy a bit lower.

Recall[3] that the minimum energy E for a knot type is at least $2\pi c$, where c is the topological crossing number. Our experiments suggest this inequality is far from sharp: the minimum of the ratio E/c seems closer to $2\pi^2$, achieved by the Hopf link 2_1^2. However, we still expect our ordering of knots by Möbius energy to list knots of small crossing number first. In fact, this is reflected in our table, though it seems that nonalternating links have significantly less energy than their crossing number would suggest—evidently two over-crossings in a row require less twisting from a three-dimensional perspective. The ordering of rational (or two-bridge) knots by our energy seems quite predictable from their Conway names (their structure as rational tangles). Indeed, for each k,

Knot or Link	$E_{\cos}$	E_{edge}	E_{vert}	A	N_{e}
0_1	0.0	0.1	−0.1	0.0	256
2_1^2	2	39.5	39.9	39.2	2.3	192
3_1	3	70.4	70.8	70.1	4.1	264
4_1^2	4	99.1	99.5	98.7	5.5	320
4_1	22	104.9	105.2	104.6	5.5	602
5_1	5	126.8	127.3	126.3	6.9	360
5_2	32	134.6	135.0	134.1	7.0	574
6_3^3	2,2,2−	136.8	137.1	136.5	6.9	534
5_1^2	212	138.9	139.3	138.4	7.1	674
6_1^2	6	154.1	154.6	153.6	8.2	584
6_1	42	162.8	163.4	162.1	8.4	640
6_2^2	33	164.5	164.9	163.8	8.4	684
7_7^2	3,2,2−	166.0	166.4	165.7	8.5	560
6_2	312	168.5	169.1	167.9	8.6	746
6_3^2	222	170.0	169.8	169.4	8.5	722
6_3	2112	172.9	173.2	172.4	8.7	914
7_8^2	21,2,2−	173.9	174.3	173.5	8.9	592
6_1^3	2,2,2	174.6	175.2	174.2	8.6	756
7_1	7	181.0	181.7	180.4	9.7	504
7_2	52	190.3	191.0	189.6	9.8	728
7_3	43	192.7	193.2	191.9	9.7	756
8_7^3	4,2,2−	194.2	194.7	193.8	9.8	612
7_1^2	412	196.6	197.2	195.9	9.9	820
8_{19}	3,3,2−	197.0	197.3	196.7	10.2	680
7_4	313	197.7	198.1	197.1	9.9	940
6_2^3	6*	197.9	198.3	197.4	9.2	492
7_3^2	232	198.7	199.1	198.0	9.8	796
7_5	322	199.7	200.0	199.0	9.9	902
8_{15}^2	22,2,2−	203.3	203.8	202.9	10.2	826
7_2^2	3112	203.6	203.8	203.2	10.1	1224
7_6	2212	203.7	204.0	203.1	10.2	970
8_8^3	31,2,2−	203.7	204.3	203.2	10.3	700
8_{20}	3,21,2−	203.9	204.4	203.4	10.4	720
7_4^2	3,2,2	204.4	205.1	203.7	10.0	808
7_1^3	2,2,2+	205.4	206.0	204.7	10.3	890
8_3^4	2,2,2,2−−	206.0	206.5	205.5	9.8	672
7_7	21112	207.1	207.0	206.5	10.2	1080
8_1^2	8	207.9	208.7	207.1	11.0	512
8_{16}^2	211,2,2−	208.2	208.5	207.6	10.3	912
7_5^2	21,2,2	208.9	209.4	208.2	10.1	916
8_{21}	21,21,2−	209.5	210.0	209.0	10.5	852
8_9^3	(2,2)(2,2−)	216.3	216.5	215.8	10.5	758
8_2^4	2,2,2,2−	217.2	217.7	216.6	10.9	752
8_{10}^3	(2,2)−(2,2)	217.4	217.7	216.9	10.6	720

Knot or Link	$E_{\cos}$	E_{edge}	E_{vert}	A	N_{e}
8_1	62	217.4	218.3	216.7	11.1	798
8_2^2	53	220.3	220.9	219.5	11.1	776
8_3	44	220.9	221.1	220.1	11.1	836
9_{43}^2	5,2,2−	221.9	224.1	223.7	11.3	1568
8_2	512	224.1	224.8	223.3	11.3	898
8_6^2	242	226.2	226.8	225.4	11.4	934
8_4	413	226.2	226.7	225.4	11.3	878
8_3^2	422	227.9	227.4	227.2	11.2	998
8_6	332	228.6	229.2	227.8	11.3	914
8_4^2	323	229.6	229.7	228.9	11.2	974
7_6^2	6*2	231.1	231.6	230.6	10.7	760
8_7	4112	231.3	231.2	230.5	11.4	880
8_8	2312	232.4	232.9	231.6	11.5	1002
8_1^3	4,2,2	232.7	233.5	231.8	11.3	862
8_9	3113	233.2	233.3	232.4	11.4	906
8_{11}	3212	233.7	233.8	232.9	11.4	1034
8_5	3,3,2	234.0	234.6	233.2	11.3	954
8_3^3	2,2,2++	234.1	234.0	233.4	11.5	1220
9_1	9	234.6	235.6	233.7	12.3	576
8_{12}	2222	235.1	234.6	234.4	11.4	1036
8_5^2	3122	235.2	235.3	234.8	11.5	1406
8_7^2	21212	237.8	237.5	237.1	11.6	1176
8_{13}	31112	237.9	238.1	237.1	11.5	982
8_{10}	3,21,2	238.7	239.3	237.9	11.5	1006
8_{14}	22112	238.7	238.7	237.9	11.6	956
8_2^3	31,2,2	238.9	239.4	238.1	11.5	900
8_{12}^2	21,2,2+	239.3	239.1	238.6	11.7	1180
8_9^2	22,2,2	239.6	240.0	238.9	11.6	1044
8_{11}^2	3,2,2+	241.6	241.3	241.2	11.6	1700
8_{10}^2	211,2,2	243.0	243.2	242.3	11.6	1114
8_1^4	2,2,2,2	243.1	243.8	242.3	11.5	844
8_{15}	21,21,2	243.1	243.0	242.5	11.7	1154
8_4^3	(2,2)(2,2)	245.8	246.5	245.1	11.5	906
8_8^2	211112	246.0	248.1	247.7	11.7	1868
8_5^3	6*3	260.5	261.2	259.8	12.0	828
8_6^3	6*2:.20	264.4	264.8	263.7	12.1	916
8_{16}	6*2.20	264.5	264.8	263.9	12.4	862
8_{14}^2	6*2:.2	264.8	265.1	264.1	12.1	894
8_{17}	6*2.2	265.1	265.7	264.4	12.3	832
8_{13}^2	6*21	266.0	266.2	265.3	12.2	998
8_{18}	8*	283.9	284.3	283.4	12.6	844
9_{31}	2111112	284.1	284.2	283.9	13.3	2616
9_{40}	9*	329.6	329.9	329.4	14.3	1640
15_1	15	394.2	395.6	392.8	20.2	1022

Table 2: Approximate Möbius energies of links through eight crossings (see text).

the lowest energy alternating k-crossing link in the table is the $(2, k)$ torus link with notation k. The highest energy two-bridge link is $21 \cdots 12$.

Many of the non-alternating links in the table have the notation $p, q, 2-$ and in each case, this link is very close in energy to $p1q$, a link with one less crossing. Note that the link $p, 2, 2-$ consists of a $(2, p)$ torus link together with the core circle of the torus which links it twice.

Suppose we look at the highest energy knots and links for a fixed number of crossings. These in general seem to be knots based (in Conway's nomenclature) on the planar diagrams 6*, 8*, etc., in which all regions have at least three sides. In fact, 6* (the Borromean rings, 6_2^3) and 8* (8_{18}), which each have significantly more energy than all others with the same number of crossings, each fit into the class of so-called "Turk's-head" knots, with very symmetric planar diagrams. The energy minimizers stay close to this plane, with the strands weaving up and down only slightly, and presumably this accounts for the high energy. The highest-energy link of seven crossings, 6*2 (7_6^2) is in fact the Borromean rings with one of the six crossings replaced by a double half-twist. It thus also has a symmetric planar picture, although we would have to apply Möbius transformations to the picture in the Appendix to see this.

We have included in the table four knots of nine crossings, which we believe to be extreme for energy. We expect that 5,2,2− (9_{43}^2) has the lowest energy of any nine crossing link. The $(2, 9)$ torus knot 9 (9_1) presumably has the lowest energy among alternating knots and links. The knot 2111112 (9_{31}) is presumably highest-energy among arithmetic nine-crossing knots. And 9* (9_{40}) should have the highest energy overall. We have also included the $(2, 15)$ torus knot to indicate the limiting helical behavior.

The Appendix shows stereo pictures of the approximate minimizer for each link. We made no particular effort to choose an optimal projection or Möbius representative for the minimizers; often, as for 7_3^2, there is some conformal symmetry that fails to be Euclidean for our representative. To see the stereoscopic effect, look at the left figure with the right eye and the right one with the left eye (by crossing the eyes). Please see our report[1] in *Geometric Topology* for a version of these pictures printed instead for straight-eyed viewing.

Acknowledgments

This research was supported in part by the NSF (Kusner) and by the Geometry Center (Sullivan), and at MSRI by NSF grant DMS-9022140. We would like to thank Ken Brakke for his help in adding features to the `evolver`, and John Conway, Peter Doyle, and Bill Thurston for useful discussions. This paper is an updated version of our report[1] in *Geometric Topology*.

Appendix

./append/0_1l.ps not found
0_1

./append/2#2_1l.ps not found
2_1^2

./append/2#2_1r.ps not found
2

./append/3_1l.ps not found
3_1

./append/4#2_1l.ps not found
3

./append/4#2_1r.ps not found
4_1^2

4

./append/5_1l.ps not found
5_1

./append/6#2_1l.ps not found
5

./append/6#2_1r.ps not found
6_1^2

6

./append/7_1l.ps not found
7_1

./append/8#2_1l.ps not found
7

./append/8#2_1r.ps not found
8_1^2

8

./append/9_1l.ps not found
9_1

./append/15_1l.ps not found
9

./append/15_1r.ps not found
15_1

15

$(2, q)$ torus knots and links

./append/4_1l.ps not found

4_1

./append/5_21.ps not found

22

./append/5_2r.ps not found

32

./append/6_1l.ps not found

6_1

./append/6#2_21.ps not found

42

./append/6#2_2r.ps not found

6_2^2

33

./append/7_2l.ps not found

7_2

./append/7_31.ps not found

52

./append/7_3r.ps not found

7_3

43

./append/8_1l.ps not found

8_1

./append/8#2_21.ps not found

62

./append/8#2_2r.ps not found

8_2^2

53

./append/8_3l.ps not found

8_3

./append/8_31.ps not found

44

./append/_r.ps not found

Rational links with two-term continued fractions

./append/5#2_1l.ps not found
5_1^2 212

./append/6#2_1l.ps not found
6_2 312

./append/6_2r.ps not found

./append/7#2_1l.ps not found
7_1^2 412

./append/8#2_1l.ps not found
8_2 512

./append/8_2r.ps not found

./append/7_4l.ps not found
7_4 313

./append/8_4l.ps not found
8_4 413

./append/8_4r.ps not found

./append/6#2_3l.ps not found
6_3^2 222

./append/7_5l.ps not found
7_5 322

./append/7_5r.ps not found

./append/8#2_3l.ps not found
8_3^2 422

./append/8#2_4l.ps not found
8_4^2 323

./append/8#2_4r.ps not found

Most rational links with three-term continued fractions

./append/7#2_3l.ps not found 7^2_3 232

./append/7#2_6l.ps not found 8^2_6 242

./append/8#2_6r.ps not found

./append/8_6l.ps not found 8_6 332

./append/8_12l.ps not found 8_{12} 2222

./append/8_12r.ps not found

./append/6_3l.ps not found 6_3 2112

./append/7#2_2l.ps not found 7^2_2 3112

./append/7#2_2r.ps not found

./append/8_7l.ps not found 8_7 4112

./append/8_9l.ps not found 8_9 3113

./append/8_9r.ps not found

./append/7_6l.ps not found 7_6 2212

./append/8_11l.ps not found 8_{11} 3212

./append/8_11r.ps not found

More rational links with three- or four-term continued fractions

./append/8#2_5l.ps not found

8^2_5 3122

./append/8#2_5r.ps not found

8_8 2312

./append/8_8r.ps not found

./append/7_7l.ps not found

7_7 21112

./append/7_7r.ps not found

8^2_7 21212

./append/8#2_7r.ps not found

./append/8_13l.ps not found

8_{13} 31112

./append/8_14l.ps not found

8_{14} 22112

./append/8_14r.ps not found

./append/8#2_8l.ps not found

8^2_8 211112

./append/8#2_9_31l.ps not found

9_{31} 2111112

./append/9_31r.ps not found

./append/8_19l.ps not found

8_{19} 3,3,2-

./append/8_19r_1.ps not found

./append/_r.ps not found

Rational links with long continued fractions, and the $(3, 4)$ torus knot

./append/6#3_1l.ps not found

6^3_1 2,2,2

./append/7#2_4l.ps not found

7^2_4 3,2,2

./append/7#2_4r.ps not found

./append/7#2_5l.ps not found

7^2_5 21,2,2

./append/8#3_1l.ps not found

8^3_1 4,2,2

./append/8#3_1r.ps not found

./append/8#2_10l.ps not found

8^2_{10} 211,2,2

./append/8#2_9l.ps not found

8^2_9 22,2,2

./append/8#2_9r.ps not found

./append/8_15l.ps not found

8_{15} 21,21,2

./append/8_10l.ps not found

8_{10} 3,21,2

./append/8_10r.ps not found

./append/8_5l.ps not found

8_5 3,3,2

./append/8#3_2l.ps not found

8^3_2 31,2,2

./append/8#3_2r.ps not found

Links with Conway notation a, b, c

./append/6#3_3l.ps not found

6^3_3 2,2,2−

./append/7#2_8l.ps not found

7^2_8 21,2,2−

./append/7#2_8r.ps not found

./append/7#2_7l.ps not found

7^2_7 3,2,2−

./append/8#3_8l.ps not found

8^3_8 31,2,2−

./append/8#3_8r.ps not found

./append/8#3_7l.ps not found

8^3_7 4,2,2−

./append/8#2_16l.ps not found

8^2_{16} 211,2,2−

./append/8#2_16r.ps not found

./append/9#2_43l.ps not found

9^2_{43} 5,2,2−

./append/8#2_15l.ps not found

8^2_{15} 22,2,2−

./append/8#2_15r.ps not found

./append/8_21l.ps not found

8_{21} 21,21,2−

./append/8_20l.ps not found

8_{20} 3,21,2−

./append/8_20r.ps not found

Most nonalternating links

./append/8#4_1l.ps not found

8^4_1 2,2,2,2

./append/8#3_4l.ps not found

8^3_4 (2,2)(2,2)

./append/8#3_4r.ps not found

./append/8#3_9l.ps not found

8^3_9 (2,2)(2,2−)

./append/8#3_10l.ps not found

8^3_{10} (2,2)−(2,2)

./append/8#3_10r.ps not found

./append/8#4_2l.ps not found

8^4_2 2,2,2,2−

./append/8#4_3l.ps not found

8^4_3 2,2,2,2−−

./append/8#4_3r.ps not found

./append/7#3_1l.ps not found

7^3_1 2,2,2+

./append/8#3_3l.ps not found

8^3_3 2,2,2++

./append/8#3_3r.ps not found

./append/8#2_11l.ps not found

8^2_{11} 3,2,2+

./append/8#2_12l.ps not found

8^2_{12} 21,2,2+

./append/8#2_12r.ps not found

The remaining links based on 1*

./append/6#3_2l.ps not found

6^3_2

./append/6#3_7l.ps not found

6*

./append/7#2_6l.ps not found

7^2_6

./append/7#2_6r.ps not found

6*2

./append/8#3_5l.ps not found

8^3_5

./append/8#3_13l.ps not found

6*3

./append/8#2_13l.ps not found

8^2_{13}

./append/8#2_13r.ps not found

6*21

./append/8_17l.ps not found

8_{17}

./append/8_16l.ps not found

6*2.2

./append/8_16r.ps not found

8_{16}

6*2.20

./append/8#2_14l.ps not found

8^2_{14}

./append/8#3_6l.ps not found

6*2:.2

./append/8#3_6r.ps not found

8^3_6

6*2:.20

./append/8_18l.ps not found

8_{18}

./append/9_40l.ps not found

8*

./append/9_40r.ps not found

9_{40}

9*

The links based on 6*, 8* or 9*

References

1. Robert B. Kusner and John M. Sullivan. Möbius energies for knots and links, surfaces and submanifolds. In Willam H. Kazez, editor, *Geometric Topology*, pages 570–604, Providence, 1997. Amer. Math. Soc./Int'l Press.
2. Jun O'Hara. Energy of a knot. *Topology*, 30:241–247, 1991.
3. Michael H. Freedman, Zheng-Xu He, and Zhenghan Wang. On the Möbius energy of knots and unknots. *Annals of Math.*, 139(1):1–50, 1994.
4. Jean-Luc Brylinski. The beta function of a knot. MSRI dg-ga preprint 97 10 011, 1997.
5. Andrzej Stasiak, Vsevolod Katritch, Jan Bednar, Didier Michoud, and Jacques Dubochet. Electrophoretic mobility of DNA knots. *Nature*, 384(14):122, November 1996.
6. Vsevolod Katritch, Jan Bednar, Didier Michoud, Robert G. Scharein, Jacques Dubochet, and Andrzej Stasiak. Geometry and physics of knots. *Nature*, 384(14):142–145, November 1996.
7. H. K. Moffatt. Pulling the knot tight. *Nature*, 384:114, November 1996.
8. Jason Cantarella, Robert B. Kusner, and John M. Sullivan. Crossing numbers of tight knots. *Nature*, 1997. To appear.
9. Lucas Hsu, Rob Kusner, and John M. Sullivan. Minimizing the squared mean curvature integral for surfaces in space forms. *Experimental Mathematics*, 1(3):191–207, 1992.
10. Thomas J. Willmore. A survey on Willmore immersions. In *Geometry and Topology of Submanifolds, IV (Leuven, 1991)*, pages 11–16. World Sci. Pub., 1992.
11. Xavier Michalet and David Bensimon. Observations of stable shapes and conformal diffusion in genus 2 vesicles. *Science*, 269:666–668, August 1995.
12. Dennis Roseman. What should a surface in 4-space look like? In Hans-Christian Hege and Konrad Polthier, editors, *Visualization and Mathematics*, pages 67–82. Springer Verlag, Heidelberg, 1997.
13. Peter Doyle and Oded Schramm. Personal communications.
14. David Auckly and Lorenzo Sadun. A family of Möbius invariant 2-knot energies. In Willam H. Kazez, editor, *Geometric Topology*, pages 235–258, Providence, 1997. Amer. Math. Soc./Int'l Press.
15. Robert B. Kusner and John M. Sullivan. A nonlocal, Möbius-invariant energy for embedded submanifolds. In preparation.

16. Kenneth A. Brakke. The Surface Evolver. *Experimental Math.*, 1:141–165, 1992.
17. Kazushi Ahara. The numerical analysis of an energy of a knot. Preprint with video, Univ. of Tokyo.
18. Steve Bryson, Michael H. Freedman, Zheng-Xu He, and Zhenghan Wang. Möbius invariance of knot energy. *Bulletin Amer. Math. Soc.*, 28:99–103, 1993.
19. Greg Buck and J. Orloff. Computing canonical conformations for knots. *Topology Appl.*, 51:247–253, 1993.
20. Greg Buck and Jonathan Simon. Knots as dynamical systems. *Topology Appl.*, 51:229–246, 1993.
21. Shinji Fukuhara. Energy of a knot. In Y. Matsumoto, T. Mizutani, and S. Morita, editors, *A Fête of Topology*, pages 443–451. Academic Press, 1988.
22. Charlie Gunn. Personal communication.
23. Terry J. Ligocki and James A. Sethian. Recognizing knots using simulated annealing. *J. Knot Theory Ramifications*, 3(4):477–495, 1994.
24. Robert P. Grzeszczuk, Milana Huang, and Louis H. Kauffman. Physically-based stochastic simplification of mathematical knots. *IEEE Trans. on Visualization and Comp. Graphics*, 3(3):262–272, 1997.
25. Allen E. Hatcher. A proof of the Smale conjecture $\mathrm{Diff}(s^3) \simeq o(4)$. *Annals of Math.*, 117:553–607, 1983.
26. John M. Sullivan. Knots minimizing a Möbius-invariant energy. VHS video tape (Nov. 1993) available from the author.
27. Colin C. Adams. *The Knot Book*. W. H. Freeman, 1994.
28. Robert B. Kusner and John M. Sullivan. On distortion and thickness of knots. In S. Whittington, D. Sumners, and T. Lodge, editors, *Topology and Geometry in Polymer Science*, IMA Volumes in Mathematics and its Applications, 103, pages 67–78, New York, 1997. Springer.
29. Richard A. Litherland, Jon Simon, Oguz Durumeric, and Eric Rawdon. Thickness of knots. Preprint, 1996.
30. Jason Cantarella, Dennis DeTurck, and Herman Gluck. Upper bounds for writhe and helicity. Preprint, 1997.
31. Greg Buck and Jon Simon. Thickness and crossing number of knots. *Topol. Appl.* to appear.
32. Greg Buck. Applications of the projection energy for knots. Preprint, 1994.
33. Denise Kim and Rob Kusner. Torus knots extremizing the Möbius energy. *Experimental Math.*, 2:1–9, 1993.

34. L. Föppl. Stabile Anordnungen von Elektronen im Atom. *J. reine angew. Math.*, 141:251–302, 1912.
35. Robert B. Kusner and John M. Sullivan. Möbius energy of Hopf links, and electrons on the sphere. In preparation.
36. Nariya Kawazumi. On the homotopy type of the moduli space of n-point sets of P^1. *J. Fac. Sci., Univ. Tokyo, IA*, 37:263–287, 1990.
37. Rob Kusner, Peter Norman, and John Sullivan. Möbius energy minimizing knot catalog. Preprint III.18, GANG/UMass Amherst, 1993.
38. Gerhard Burde and Heiner Zieschang. *Knots*. Number 5 in Studies in Math. de Gruyter, Berlin, 1985.
39. Dale Rolfsen. *Knots and Links*. Publish or Perish, Wilmington, 1976.
40. John H. Conway. An enumeration of knots and links and some of their related properties. In J. Leech, editor, *Computational Problems in Abstract Algebra*, pages 329–358. Pergamon, 1970. Proc. Conf. Oxford, 1967.